The Cross Section for the Photodetachment of Electrons from I^-*

Bruce Steiner
National Bureau of Standards,
Washington, D.C. 20234
(Received 15 April 1968)

The cross section for photodetachment of I^- at 347 nm, 0.5 eV above threshold, has been determined to be $(2.9 \pm 0.5) \times 10^{-17}$ cm^2. This value has been obtained in a crossed-beam experiment by comparison with photodetachment from H^- at 993 nm, 0.5 eV above *its* threshold. The present determination permits placement of the previously determined relative-cross-section curve for the first electron volt above threshold on an absolute scale. The entire experimental curve is compared with the recent calculation of Robinson and Geltman. Although the shapes of the two curves are very similar, the new experimental cross section exceeds the calculation by nearly a factor of 2.

INTRODUCTION

The distribution of energy in the solar spectrum is known to be determined by the H^- continuum.[1] Although the dominant factors in the continua of other stars have not yet been identified, the projected elemental abundances and temperatures indicate that heavier negative ions may control the spectra of other stars in a manner analogous to that of H^- in the sun.[2,3] Firm understanding of the role of individual negative ions in such stellar spectra requires the photodetachment cross sections.

In the *D* region of the earth's ionosphere, the diurnal variation of the electron density associated with polar-cap absorption events has been ascribed to attachment of electrons to form negative ions at sunset and subsequent detachment at sunrise.[4–9] However, neither of the particular negative ions thought to be present, O^- and O_2^-, have electrons bound with the energy necessary to explain the observations. Both electron affinities and absolute cross sections for heavy atomic and molecular negative ions are required for evaluation of models for the physics of the *D* region.

In the laboratory, a potential source for slow, monoenergetic, well-collimated atomic and molecular beams can be visualized in the photodetachment of negative-ion beams. Such a source would not involve the energy and angular broadening inherent in charge transfer from positive-ion beams. Determination of the feasibility of such an approach rests on knowledge of photodetachment cross sections.

In spite of the usefulness of the knowledge of photodetachment cross sections, few have been determined experimentally[10–15] or theoretically.[16–22] In fact a recent calculation of the single-quantum photodetachment cross section[23] of I^- represents the first attempt to calculate a photodetachment cross section for a negative ion beyond the second row of the periodic table. The agreement of the shape of this cross section over a region one electron volt above the threshold with the experimental relative cross section[24] is remarkably good (Fig. 1). The uncertainty in the calculations is difficult to estimate from internal considerations alone. However, if the present experiment confirms the absolute magnitude of the calculations, such agreement would suggest that present theory may be adequate for the calculation of the photodetachment cross sections for most of the atomic negative ions of the periodic table.

Furthermore, the cross section for the single-quantum photodetachment of I^- is of particular interest in connection with recent experiments on the double-quantum photodetachment of I^-.[25] The theoretical estimate[26] of the double-quantum cross section was substantially lower than the experimental value. The double-quantum theoretical estimate of the cross section was based, however, in turn on the experimentally determined single-quantum cross section.[27] If the resulting double-quantum estimate is in fact in error, the error could be due at least in part to error in the experimental single-quantum cross section upon which the theory is based rather than to the theory itself. A new determination of the single-quantum cross section will shed light on this question.

The behavior of the cross section for I^- as a function of energy above threshold has been studied previously by both shock-wave[14–15] and crossed-beam[24] techniques. Although the relative cross section shape was rather precisely determined in these experiments, the absolute magnitude of the cross section was much less well determined.[14,15,27] The present experiment was performed to determine the absolute magnitude of the cross section at

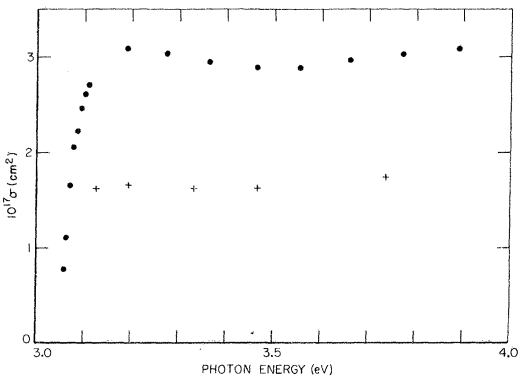

FIG. 1. Previous experimentally determined relative cross section[24] normalized by present results (●) and theoretical results of Geltman[23] (+).

347 nm, 0.5 eV above threshold, with sufficient precision and accuracy to permit meaningful comparison with theory.

APPROACH

A cross section can be determined, of course, in one of two manners: (1) by measuring all quantities involved absolutely – light intensity, ion current, and photodetached electron current; or (2) by accurate comparison of the ratios of these quantities with those for another photodetachment process whose cross section is well known. The first method requires considerably greater effort than the second; the additional effort is justified only if no suitable cross section for comparison exists.

The photodetachment cross section for H^- has been calculated by a number of different workers with a variety of wave functions employed in the different "length", "velocity", and "acceleration" formulations. The various formulations will give identical results if sufficiently accurate wave functions are used. Although similarity of results of the three formulations is not proof of sufficient accuracy, such similarity implies that the results are most probably not seriously in error. This implication is strengthened in the case of H^- by the observation that various nonidentical wave functions give similar results. Thus John[19] employed Hylleraas-type Hart and Hertzberg bound-state wave functions and $1s$-exchange-approximation continuum functions. Later, Geltman[18] obtained essentially similar "dipole"-form cross sections with Schwartz bound-state functions and variationally determined continuum functions containing excited states of the hydrogen atom, and in addition, his "length"-formulation calculation was significantly closer to the "dipole" form than was the "length" formulation of John. Most recently Doughty, Fraser, and McEachran[17] also have achieved similar "dipole" results with Hartree-Fock continuum functions and the Schwartz bound-state functions. Their "length"- and "acceleration"-form calculations display further approach to the "dipole" results. In summary, as the wave functions are steadily refined so that the three formulations give results approaching one another, the "dipole"-formulation results themselves show very little change indeed. Since the various "dipole"-formulation results between 400 and 1000nm agree well within the few-percent accuracy of the present experiment, and since the theoretical cross section falls within the 10% uncertainty ascribed to the experimental H^- cross section, the H^- cross section is taken to be sufficiently well established to serve as an absolute standard. The cross section for photodetachment from I^- therefore has been determined by comparison with that for H^-.

The photodetachment probability, or ratio of the photodetached electron current i_e to the negative-ion current i_i is given by the product of the cross section to be determined σ, the photon flux ρ, and the time t which the negative ion spends in the photon beam, and a geometrical overlap factor f which specifies the degree of overlap of the ion beam and light beam in their common dimension h:

$$i_e/i_i = \sigma\rho t f,$$

$$f = \int \rho(h) \left(\frac{di_i(h)}{dh}\right) dh \Big/ \int \left(\frac{dp(h)}{dh}\right) dh \int \left(\frac{di_i(h)}{dh}\right) dh.$$

The quantity to be determined in the present experiment, the ratio of the cross section for photodetachment of I^- to that for H^-, is therefore given by the product of various experimentally measured ratios:

$$\sigma_{I^-}/\sigma_{H^-} = (i_{eI^-}/i_{eH^-})(i_{iH^-}/i_{iI^-}) \times (\rho_{H^-}/\rho_{I^-})(t_{H^-}/t_{I^-})(f_{H^-}/f_{I^-}). \quad (1)$$

This comparison may be made in at least two different ways. Past experiments have been performed at a single wavelength. Alternatively, however, the measurements may be performed at different wavelengths for the two ions so that each measurement is made at a constant energy above threshold.

If the comparison of the cross sections is made at a single wavelength, the initial energies of the two photodetached electron beams will not be identical, partly because of the difference in threshold energies (electron affinities), 2.31 eV, and partly because of the difference of 1.36 eV caused by detachment from ions of different velocity (Doppler effect). The angular distribution of initial velocities arising from the former effect will depend both on the polarization of the light and the nature of the transition involved[28,29]; the component of the initial velocities from the latter effect will be directed along the ion beam. The trajectories of the electrons through the lenses used to collect the detached electrons therefore will change appreciably in switching from I^- to H^-. On the other hand, comparison at two different wavelengths, each a fixed amount in energy above the threshold for detachment of the ion in question, reduces the difference in energy of the electrons from the two ions. Appropriate relocation of the region of interaction of the ion and photon beams (Fig. 2) further reduces the difference in trajectories of the electrons from I^- and H^-. This relocation is achieved by translation of the light beam so that the electrons remain near the axis of the electron lens. Such a procedure requires knowledge concerning the wavelength dependence of certain parameters, of course: the transmission of the quartz and sapphire windows, the reflectivity of the black thermopile coating, and the geometrical beam-overlap factor. But variation in these parameters is considered to be more accurately measured than are the effects of severe dislocation of the electron trajectories. The comparison of the cross sections therefore has been made 0.5 eV above each threshold: 347 nm for I^- and 993nm for H^-.

INSTRUMENT

The instrument consists of an ion source and

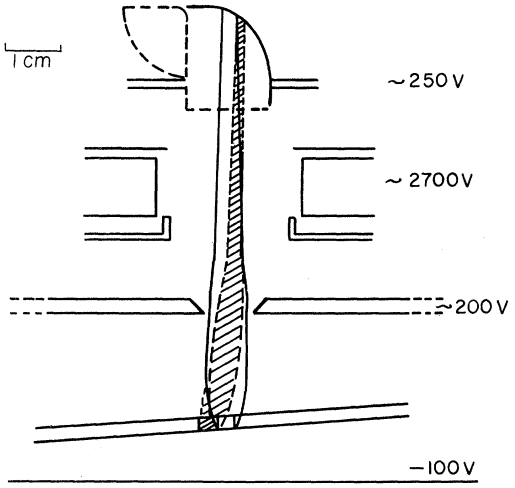

FIG. 2. Schematic of interaction chamber showing the nearly horizontal ion and vertical electron beams from I^- (clear) and H^- (shaded). The photon beam is focused onto the clear rectangular area of the I^- beam near the vertical symmetry axis, and onto shaded rectangular area of the H^- beam. The top and bottom field-defining plates (~200 and -100 V respectively) are separated by 3 cm.

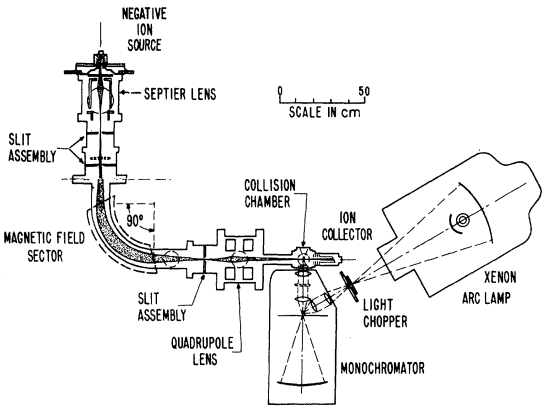

FIG. 3. Arrangement of ion-beam and photon-beam optics.

sector-field magnetic mass analyzer, a light source and monochromator, and collection optics and multiplier for the detached electrons (Figs. 3 and 4). I^- and H^- ions were formed in a magnetically confined, hot-cathode arc discharge through a mixture of iodine and ammonia vapor in a source similar to the one employed by Seman and Branscomb.[13] Negative-ion beams of approximately 10^{-8} A were extracted from the source by a Septier lens[30] and focused onto the entrance slit of a 12-in (30-cm) sector-field mass analyzer. The full mass resolution of 1/300 with 1/2-mm slits was degraded to 1/60 by the spread in energy of the ions emerging from the source. HI^- was not observed under these conditions nor was it anticipated, because of its closed-shell–plus–one structure. Ions emerging from the exit slit of the mass analyzer were focused by a quadrupole lens onto a rectangular area 1.6 mm × 2.5 mm.

Light from a commercial high-pressure arc-discharge lamp was chopped at 2160 Hz and resolved by an $f/1.5$ monochromator. Auxiliary slits limited the size of the light beam to an area only slightly larger than that traversed by the ion beams. In the monochromator, a beam splitter took approximately 10% of the resolved light for monitoring by a thermopile throughout the experiment. The ratio of power in the monitored beam to that in the main beam as a function of wavelength was determined in a separate experiment by identical thermopiles constructed for this purpose. For the 10 nm resolution (full width at half height) of this experiment, the photon image size was limited to an area approximately 3.5 mm × 2 mm at the focus. The electrons formed in the region of intersection of these two beams, approximately 1.6 mm × 2.5 mm × 2.0 mm were accelerated by a uniform field of 100 V/cm into an electron lens which focused the beam onto the first dynode of an electron multiplier. The signal from the multiplier was amplified and detected at the chopping frequency by a phase-sensitive amplifier.

SYSTEMATIC UNCERTAINTIES

The measurement of the ratios in Eq. (1) is subject to a variety of systematic uncertainties which will seriously affect the final accuracy of the cross-section determination. An attempt has been made to determine the extent to which uncertainty in each measurement affects the final results.

Electron Currents

It must be assured that essentially all photodetached electrons enter the multiplier and are recorded with known efficiency. Since we know both the location of the region in which the electrons are detached and the ambient field, we can calculate the trajectories below the slit entrance (Figs. 2, 4). Under the conditions of the experiment, all electrons detached along a 3-mm equipotential line in the 100-V/cm field will pass the 7-mm aperture located 5.1 mm away. Transmission of the electrons has been verified by closing the aperture and observing the attenuation of the electron current. Within the measurement uncertainty of 1%, all photodetached electrons are transmitted by the slit. Model calculations for the lens performance between the slit and the electron multiplier indicate that the lens should perform approximately as desired. Electrons from I^- formed close to threshold have been utilized to form a small beam for scanning across the multiplier surface and observing its response (Fig. 5). The relative gain of the multiplier as a function of location has thus been determined. A combination of lateral translation of the source of electrons by translation either of the ion beam or

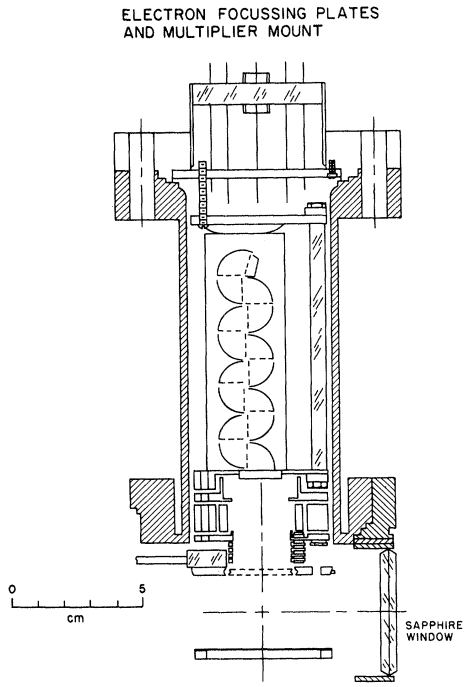

FIG. 4. Electron optics shown in plane perpendicular to that of Fig. 1. Photons enter through window at right; ions enter drawing perpendicular to it in the vicinity of +, to the left of the window.

of the photon beam and scanning the electrons across the multiplier permits one to examine the lens behavior in detail and thus to verify the behavior of the model lens calculations.

As noted above, although the electrons from both H^- and I^- carried away the 0.5-eV energy transmitted by the photons 0.5 eV above threshold, the H^- electrons carried away a much greater fraction of the 2500-eV kinetic energy of the ion than did the I^- electrons. For the comparison of the present experiment, the electrons from H^- therefore were formed 3 mm "upstream" from the region of formation of the I^- electrons (Fig. 2). Thus they clear the slit discriminating against other electrons and follow generally more similar trajectories. Since the spatial spread of the electrons from H^- was somewhat less than that of the I^- electrons, the precision of this 3-mm translation was uncritical. The translation of the beam at the multiplier, corresponding to a translation of the electron "source," was calculated to be to approximately 10% of the full width of Fig. 4. The ratio of the I^- and H^- electron current was corrected for the 4.5% decrease in multiplier gain, and a conservative uncertainty has been taken to be the same size as the correction.

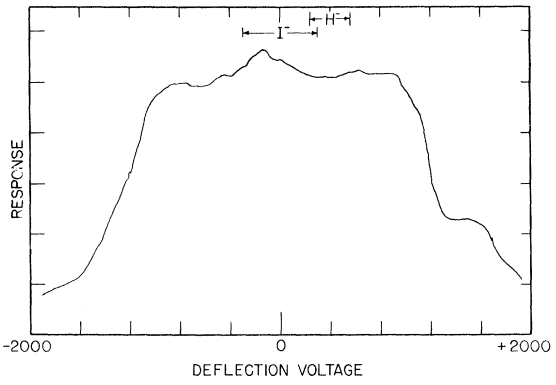

FIG. 5. Response of electron multiplier as a function of position of entry of electrons on the first dynode. Locations of impingement of electrons from the two ion beams are noted.

Ion Currents

The ion currents are measured with a Faraday cup preceded by several sets of split repeller electrodes. These electrodes serve three functions: (1) to decrease the effect of the electron collecting field on the ion trajectories; (2) to scan the ion beam across the bottom of the Faraday collector in order to test for elastically reflected ions[31]; and (3) to return low-energy secondary electrons to the Faraday collector.

Low-energy secondaries were studied by varying the voltage on the electrode immediately preceding the collector. Increasing the repeller voltage from 0 to −15 V increased the measured ion current about 5%, but no further increase in voltage affected the measured current by more than the measurement uncertainty of $\frac{1}{2}$%. This electrode was maintained at −22 volts throughout the experiment.

Scanning the beam across the sloping bottom of the Faraday collector permits one to place an upper limit of the order of $\frac{1}{2}$% on the elastically reflected ion current. The results of this test were confirmed by deflecting the beam at the entrance to the collector with a small magnet. A magnetic field sufficiently large to deflect the H^- beam from the entrance did not noticeably increase the measured ion current.

Photon Flux

The conversion of measured power in the photon beams at two different wavelengths to photon flux contains four wavelength-dependent factors: (1) the conversion of energy to number density: $(\lambda_{H^-}/\lambda_{I^-})$; (2) the ratio of power in the main beam to that in the monitored beam at the two wavelengths; (3) the photon-monitor quartz-window transmission at the two wavelengths; and (4) the transmission at the two wavelengths of the sapphire window of the interaction chamber.

The wavelengths are sufficiently well known that the first ratio contributes negligibly to the uncertainty.

The ratio of the fraction taken by the monitor-beam splitter at the two wavelengths was determined by placing identical thermopiles at the main image and monitor image. It was of more than passing interest that this ratio, although smoothly

varying with wavelength, displayed structure. This structure implies that the photon beams were appreciably polarized. Since the direction of detachment is a function of the polarization of the light as well as of the nature of the transition involved,[28,29] the angular distribution of the detached electrons varies in an undetermined way with wavelength. However, the previous arguments concerning total collection and accurate measurement of the electron beams were based on the assumption of least-favorable angular distributions. The indeterminacy of the photon polarization thus does not increase the uncertainty in the measured electron currents, and hence knowledge of the polarization of the light is not required.

With the $f/1.2$ optics employed,[32] the differential transmission with wavelength for the interaction chamber window as measured at NBS varied approximately 2% over the solid angle. The average was taken and a 1% uncertainty placed on it. The quartz thermopile window however was hemispherical so that all rays entered essentially perpendicular to its surface. The transmission as a function of wavelength was supplied by the manufacturer and an uncertainty of 1% ascribed to the ratio at the two wavelengths. The black coating was stated by the manufacturer to be independent of wavelength to within 1% and was considered to contribute negligibly to the uncertainty.

Interaction Time

The ratio of the time spent in the light beam is given, for ions of equal energy, by the ratio of the square roots of the masses: $M_{I^-}^{-1/2}/M_{H^-}^{-1/2}$ This factor is so accurately[33] known that it does not increase the uncertainty in the determination of the cross section. Although the kinetic energy of the two ion beams was not directly measured, an upper limit of the difference in this energy is probably the spread in energy of the individual beams, less than 1%. Since the interaction time is influenced only as the square root of the energy, it is considered to contribute negligibly to the uncertainty.

Beam Overlap

The beam-overlap factor derives primarily from the known nonuniformity of the light beam, which varies with wavelength, and the finite uncertainty in the uniformity of the ion beam. In addition, the translation of the light beam between the I^- and H^- measurements also enters since the electrostatic field in the interaction region is sufficiently strong that the ion beam deviates from a horizontal plane: The different ion beams traversed slightly different regions of the photon beam. Thus, vertical ion-beam displacement of 0.34 mm was associated with the horizontal light-beam displacement of 3.0 mm. The vertical variation of the light-beam intensity at the necessary wavelengths was measured first with a thermopile and later with a phototube, both fitted with slits (Figs. 6 and 7). The ion beam was explored by inserting a luminescent screen and observing the attenuation of the ion-beam current as

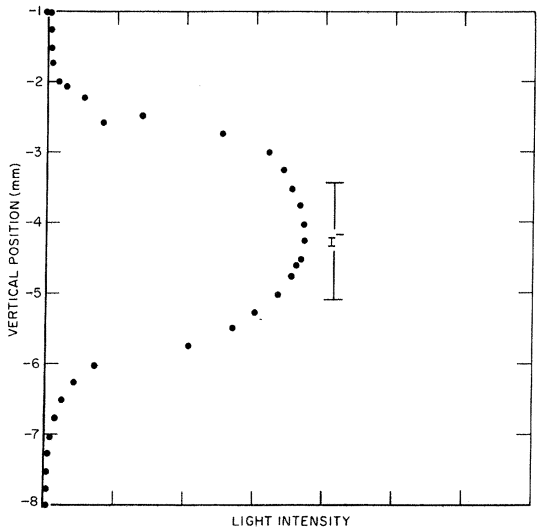

FIG. 6. Vertical distribution of 347 nm light intensity; the part traversed by the I^- beam is marked.

the screen was gradually inserted. The ion beam was thus determined to be uniform within 10%. Since the light intensity is uniform to about 10% in the region of overlap, the uncertainty in overlap due to uncertainty in ion-beam uniformity is thus of the order of 1% and is considered to be negligible. The 0.34-mm difference (20%) in vertical position of the two ion beams and the change in the form of the light beam with wavelength (Figs. 6 and 7) were calculated to require a 22.5% beam-overlap correction of the resulting electron signal. Mislocation of either of the ion beams by 1 mm would not change this factor by more than one-fourth of the correction, or 5.6%. The uncertainty in the beam-overlap factor is taken to be 5.4%.

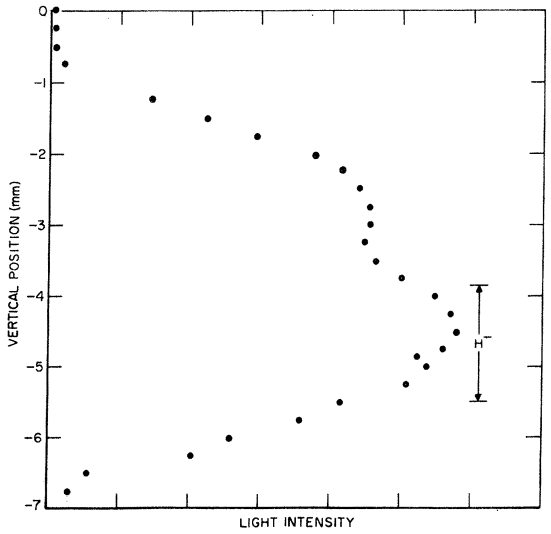

FIG. 7. Vertical distribution of 993 nm light intensity; the part traversed by the H^- beam is marked.

The agreement of the three separate determinations of the cross section within the standard deviations of their mean implies that any important fluctuations in the beam overlap are statistical in nature and can be taken to be included in the uncertainty ascribed to reproducibility.

EXPERIMENTAL RESULTS

The uncertainties discussed above are independent and quite conservative, and hence are unlikely to add linearly in contributing to the total systematic product of the measured ratios to the ratio of the cross section is 0.1470 ± 0.0115. The uncertainty is the square root of the sum of the squares of the uncertainties outlined above and an additional 2% for uncertainty in linearity. The measured ratio of cross sections as determined on three separate days over a period of one month is given in Table I. N and M are the number of observations of I^- and H^- respectively on each day.

TABLE I. Experimental determination of the ratio $\sigma_{I^-}/\sigma_{H^-}$ on different days with the number of individual determinations on each day.

$\sigma_{I^-}/\sigma_{H^-}$	Standard deviation	N	M
0.779	0.075	8	6
0.732	0.047	5	8
0.767	0.029	6	12

The uncertainties here represent the standard deviation of the reported ratios based on the propagation of error formula.

As noted above, the three most recent theoretical values of the cross section for photodetachment of H^-[17-19] agree with one another within 1% over most of the energy range and with experiment within the experimental uncertainty of 10%. The value of Geltman at 993 nm, essentially identical to those of Doughty, Fraser, and McEachran and of John, is 3.74×10^{-17} cm^2. Combining this cross section with the present data leads to a value of $(2.9 \pm 0.4) \times 10^{-17}$ cm^2 for the photodetachment cross section of I^- at 347nm, 0.5 eV above threshold. This uncertainty assumes the H^- cross section to be exact and is calculated by taking the square root of the sum of the squares of systematic uncertainties and three standard deviations of the mean. This value is to be compared with the filter determination[27]: $(2.1 \pm 1.1) \times 10^{-17}$ cm^2. Combining the 10% uncertainty of the cross section of H^- with the 7.8% systematic uncertainty and 11.4%, three times the standard deviation as the square root of the sum of the squares leads to a cross section for I^- at 347_{nm} of $(2.9 \pm 0.5) \times 10^{-17}$ cm^2. This number best represents the present experimental results; it has been used along with the previous relative cross section[24] to construct Fig. 1.

This value at 347nm can now be used to place the previously determined relative cross section[24] on an absolute scale (Fig. 1). The relative-cross-section curve, however, was not measured with the same attention to sources of systematic error of the present experiment. Hence, the accuracy of the present normalized curve is, in the strictest sense, undetermined away from the normalization point. Nevertheless, the fact that the present measurement is within the 50% uncertainty of the previous crossed-beam value[27] can be construed to imply that the relative-cross-section curve, determined by the same charged-particle optics as used in the determination of the previous absolute value, is probably not in error by more than this amount. In fact, the major uncertainty in the previous absolute value, in retrospect, is probably associated with the rather large difference in electron energies involved (more than 3 eV). Since the points on the present normalized curve represent at most an energy of 0.5 eV different from that of the normalizing point, the total error is perhaps not much more than that of the calibration point itself, ± 19%.

This determination is nearly twice the recent theoretical I^- calculation,[23] and indicates that possibly for heavy negative ions, the determination of photodetachment cross sections has not yet achieved the reliability demonstrated for the first-row negative ions.

ACKNOWLEDGMENT

It is a pleasure to acknowledge discussions with Lewis Branscomb, John Simpson, and Chris Kuyatt concerning the design of the apparatus and various aspects of the experiment. Without the able collaboration of Nikita Wells, the apparatus could not have been constructed.

*This research was supported by the Advanced Research Projects Agency of the Department of Defense under Project DEFENDER.

[1]A. Unsöld, Physik der Sternatmosphären (Springer-Verlag, Berlin, 1955).

[2]L. M. Branscomb and B. E. F. Pagel, Monthly Notices Roy. Astron. Soc. 118, 258 (1958).

[3]M. S. Vardya, Mem. Roy. Astron. Soc. 71, 249 (1967).

[4]D. R. Bates and H. S. W. Massey, J. Atmospheric Terrest. Phys. 2, 1 (1952).

[5]D. R. Bates and H. S. W. Massey, J. Atmospheric Terrest. Phys. 2, 253 (1952).

[6]J. A. Ratcliffe, Physics of the Upper Atmosphere (Academic Press Inc., New York, 1960), p. 413.

[7]L. M. Branscomb, Ann. Geophys. 20, 88 (1964).

[8]Bengt Hultqvist, Ann. Geophys. 22, 235 (1966).

[9]E. A. Lauter and R. Knuth, J. Atmospheric Terrest. Phys. 29, 411 (1967).

[10]L. M. Branscomb and S. J. Smith, Phys. Rev. 98, 1028 (1955).

[11]S. J. Smith and D. S. Burch, Phys. Rev. 116, 1125 (1959).

[12]L. M. Branscomb, D. S. Burch, S. J. Smith, and S. Geltman, Phys. Rev. 111, 504 (1958).

[13]M. L. Seman and L. M. Branscomb, Phys. Rev. 125, 1602 (1962).
[14]R. S. Berry, C. W. Reimann, and G. N. Spokes, J. Chem. Phys. 37, 2278 (1962).
[15]R. S. Berry and C. W. Reinmann, J. Chem. Phys. 38, 1540 (1963).
[16]For the most recent H^- calculations, see Refs. 17-19; for the most recent O^- calculations, see Refs. 20-21; for C^-, see Ref. 22.
[17]N. A. Doughty, P. A. Fraser, and R. P. McEachran, Monthly Notices Roy. Astron. Soc. 132, 255 (1966).
[18]S. Geltman, Astrophys. J. 136, 935 (1962).
[19]T. L. John, Monthly Notices Roy. Astron. Soc. 121, 41 (1960).
[20]R. J. W. Henry, Phys. Rev. 162, 56 (1967).
[21]W. R. Garrett and H. T. Jackson, Jr., Phys. Rev. 153, 28 (1967).
[22]V. P. Myerscough and M. R. C. McDowell, in Proceedings of the Sixth International Conference on Ionization Phenomena in Gases, Paris, 1963, edited by P. Hubert and E. Crémieu-Alcan (European Atomic Energy Community, 1964), Vol. I, p. 135.
[23]E. J. Robinson and S. Geltman, Phys. Rev. 153, 4 (1967).
[24]B. Steiner, M. L. Seman, and L. M. Branscomb, Atomic Collision Processes, edited by M. R. C. McDowell (North-Holland Publishing Co., Amsterdam, 1964) p. 537.
[25]J. L. Hall, E. J. Robinson, and L. M. Branscomb, Phys. Rev. Letters 14, 1013 (1965).
[26]S. Geltman, Phys. Letters 4, 168 (1963).
[27]B. Steiner, M. L. Seman, and L. M. Branscomb, J. Chem. Phys. 37, 1200 (1962).
[28]J. Cooper and R. N. Zare, J. Chem. Phys., 38, 942 (1968).
[29]J. L. Hall and M. W. Siegel, J. Chem. Phys., 38, 945 (1968).
[30]Albert Septier, CERN Report No. CERN 60-39, 1960 (unpublished).
[31]P. Mahadevan, G. D. Magnuson, J. D. Layton, and C. E. Carlson, Phys. Rev. 140, A1407 (1965).
[32]The aperture of the optics as determined by external angle was $f/1.2$; the aperture as determined by light-collecting solid angle was $f/1.5$.
[33]J. H. E. Mattauch, W. Thiele, and A. H. Wapstra, Nucl. Phys. 67, 1 (1965).

Hyperfine Contact Interactions in Oxygen Calculated by Many-Body Theory

Hugh P. Kelly
Department of Physics,
University of Virginia,
Charlottesville, Virginia
(Received 15 April 1968)

Many-body perturbation theory, which has been used in previous atomic calculations, is applied to the calculation of the hyperfine contact interaction in the oxygen atom. Large cancellations have been found to occur between different types of diagrams. Both core polarization diagrams and also diagrams representing electron correlations have been found to contribute significantly. The final value for $|\Psi(0)|^2$ is in good agreement with that measured by Harvey.

I. INTRODUCTION AND REVIEW

Many-body perturbation theory, as developed by Brueckner[1] and Goldstone,[2] has been applied to the calculation of many atomic properties such as correlation energies, polarizabilities, and shielding factors.[3-6] The same methods developed to calculate these properties are used in a straightforward manner in this work to calculate the hyperfine contact interaction in the oxygen atom. These methods have also been used recently to calculate the hyperfine contact interaction of the lithium atom.[7]

The contribution of the Fermi contact hyperfine term to the Hamiltonian is given by[8]

$$2\mu_I\mu_0 \sum_{i=1}^{N} \frac{8\pi}{3}\delta(\vec{r}_i)\vec{s}_i\cdot\vec{I}, \tag{1}$$

where μ_I is the nuclear magnetic moment, μ_0 is the Bohr magneton $e\hbar/2mc$, and $\vec{I}$ is the nuclear spin. The first-order contribution of Eq. (1) to the energy may be obtained by evaluating

$$\langle\psi_0|\sum_{i=1}^{N} s_{zi}\,\delta(\vec{r}_i)|\psi_0\rangle/\langle\psi_0|\psi_0\rangle \tag{2}$$

for the ground-state wave function $|\psi_0\rangle$ which is an eigenstate of L^2, S^2, L_z and S_z with eigenvalues $M_L = +L$ and $M_S = +S$. Introducing the normalized state $|LS, M_S = S\rangle = |\psi_0\rangle/(\langle\psi_0|\psi_0\rangle)^{1/2}$, we can relate Eq. (2) to the reduced matrix element[9]

$$\langle LS||\textstyle\sum_i \delta(\vec{r}_i)\vec{s}_i||LS\rangle = \langle LS, M_S = S|\sum_i \delta(\vec{r}_i)s_{zi}|LS, M_S = S\rangle \times \sqrt{3}/(SSS - S|SS10), \tag{3a}$$

where $(SSS - S|SS10)$ is a Clebsch-Gordan coefficient.[9] For oxygen, which has a ^3P ground state ($L = 1, S = 1$), this coefficient is $2^{-1/2}$.